Environ Earth Sci (2013) 70:2817–2825
DOI 10.1007/s12665-013-2341-z

ORIGINAL ARTICLE

Analysis of the bedding landslide due to the presence of the weak intercalated layer in the limestone

Baotian Xu · Changhong Yan · Song Xu

Received: 3 February 2012 / Accepted: 21 February 2013 / Published online: 9 March 2013

Abstract Analysis and research results show that the sliding plane of Jiudingshan landslide is along the weak intercalated layer (clay-filled) in the limestone and the sliding block is separated by the tension crack on the slope crest. The earlier study results show that for the rough, ups and downs structural plane, when i is greater than 2.0, the shear strength of the structural surface is intensely close to the strength of the filling. By the earlier theory, this failure must be through the clay filling. In this study, the failure is back-analyzed and the shear strength of the infilling is tested by the laboratory direct shear tests for which samples were retrieved in the field. The failure cannot be explained by the laboratory results of shear strength parameters. To simulate the field conditions, the real strength parameters of sliding surface are measured by the in situ shear tests for the weak intercalated layer. By the in situ tests, it is shown that the failure initiates along the contacts between the clay infilling and the limestone boundaries, but not through the clay itself. Though the contact surface is the interface of the clay–limestone, the cohesion is not 0 and it is not negligible too.

Keywords Bedding landslide · The weak intercalated layer · Shear strength · Back analysis

Introduction

Many studies and practices show that the weak layers have significant impact on the stability of the stratified rock mass from the analysis by the large number of projects. The stability of a rock slope, when containing an inclined plane of weakness, has been discussed by many authors (Terzaghi 1962; Jaeger 1971; Goodman 1976; Goodman and Gen 1985; Okubo and Nishiatsu 1993; Hatzor 1997). In addition, case studies have been carried out on cut slopes in Jordan, concluding that slide movements always coincided with weak layers (Alhomoud and Tubeileh 1998).

A separated block is the primary condition for rock instability, which means there is the separation surface as the side border of the instable block in the rock mass, and which has little sliding resistance; the inclination of sliding plane must be consistent with inclination of the slope. Secondly, the dipping angle of the sliding plane must be less than the slope angle of inclination and greater than the internal friction angle on the sliding plane. When the sliding force of the sliding plane is greater than resistance sliding force, the rock block will fail. According to the Mohr–Coulomb theory, the resistance sliding force depends on the strength parameters c and ϕ of the sliding plane.

The earlier study results (Barton 1971, 1973; Barton and Bandis 1982; Patton 1966; Ladanyi and Archambault 1977; Saeb and Amadei 1992; Maksimovic 1996; Grasselli and Egger 2003; Haberfield and Johnston 1994; Indraratna and Haque 2000; Kodikara and Johnston 1994; Ghazvinian and Taghichian 2010) show that for the rough, ups and downs structural plane, when the value of i (the filling thickness/the evaluation of the ups and downs of the structural surface) is greater than 1.0, the shear strength of filled surface is governed by the strength of the filling material. When i is greater than 2.0, the shear strength of the structural surface is intensely close to the strength of the filling. Hatzor (1997) pointed out that the strength of the filling clay may be greater than the contact of the clay–limestone, but the

B. Xu (✉) · C. Yan · S. Xu
School of Earth Science and Engineering, Nanjing University, Nanjing 210093, Jiangsu, China
e-mail: xubt@nju.edu.cn

strength on the contact is mainly governed by the effective internal friction angle; the cohesion is negligible.

Each slope failure process along the discontinuities in rock mass can be reasonably accounted as a large-scale in situ shear tests. On the other hand, failure zones of rock masses induced by excavation can be measured easily and reliably. Therefore, the back analysis techniques have always been a hot research topic since the 1970s and extensive studies have been conducted to develop different models of back analysis (Sakurai and Takeuchi 1983; Gioda and Locatelli 1999; Zhang et al. 2006). Back analysis has been used also based on field measurements of strains or stresses (Kaiser et al. 1990). The shear strength parameters obtained by back analysis of slope failure should be more reliable than the results obtained by laboratory, because of the influences of scale effect (Mostafa et al. 2010).

The shear strength parameters of a failed slope have been back calculated in the following procedure: assuming the value of the angle of internal friction ϕ or of the cohesion c to calculate another (Fookes et al. 1977). Assuming that the material of the sliding plane obeys Mohr–Coulomb failure criterion; therefore, the results of back analysis provide a range of combination of apparent friction angle and cohesion, which brings difficulties to the parameter selection. The above difficulties usually can be solved by utilizing two cross sections in a failed slope to establish two equations and evaluate the values of ϕ and c; the continuous curves corresponding to the two equations may have an intersection point, which represents the values ϕ and c of the sliding plane. The second method seems maybe more efficacious; however, if the range or volume of a slope failure is relatively small, the shapes of sliding blocks in different cross sections drawn from the failed zones are similar. The two continuous curves may be very approximative or overlapped; the back analysis procedure goes back to the first procedure.

Jiudingshan landslide is located in discontinuous media and the failure of rock mass is mainly controlled by the discontinuity distribution. In this study, on the basis of engineering geological investigation and survey for Jiudingshan landslide, it can be found that the failure of the landslide initiates along the weak intercalated layer, which is filled with clay. To measure the shear strength parameters on the sliding plane, the failure is back-analyzed. The shear strength of the infilling (clay) is tested by laboratory tests. To simulate the field conditions, the in situ direct shear tests are carried out. Due to the differences between the tests and back analysis, the discussion is made to determine where the sliding plane is (the sliding plane is through the filling or on the contact between the clay filling and the limestone boundaries). The ultimate strength parameters of the sliding plane are determined by contrast analysis. The accuracy of the conventional and earlier study results for the weak intercalated layer is discussed.

Background

Jiudingshan slope is located in the east of Laiwu City, at a distance of about 20 km from the city center (Fig. 1). The site is located in the southeast fringe of Laiwu Basin, which is characterized by hilly landscape, V-shape valleys, and the ground evaluation is about 300–480 m. The length and height of the slope are 100.0 m and 12.00–40.00 m, respectively. Because of construction of the new plants of Laiwu Iron & Steel Co., Ltd., the slope was excavated; after excavation, the slope angle is above 70° and the distance between slope toe and wall of new plants is 3.5–6.0 m (Fig. 2).

The Cambrian Fengshan group (ϵ_3f), which is widely exposed in the study area, comprises mainly limestone (Fig. 2), characterizes moderately to intensely weathered, gray, with strike of 280°–310°, dip direction of NE and dipping angle of 25°–40°, in which RQD is about 40–80, and the rock quality is mid-poor. The thickness of the top intensely weathered is about 10 m; the lower is moderately weathered. Locally, quaternary loess covers part of the slope, comprises mainly rubble and soil which is the weathering residues of the limestone, with a thickness of about 0–0.5 m.

Scanline surveys were carried out in the failed and adjacent zones; the range is limited by the site condition to be 3 m × 20 m along the strike of slope. The orientation and characteristics of 68 joints are collected from the clinohedron. The main discontinuities in the rock mass include two joint sets and stratification planes of the limestone (Fig. 3). Joint sets 1 (JS1) and 2 (JS2) are all sub-vertical, with strike of 300°–320° and 0°–20°, dip direction of SW and NW, dip angle of about 70°–80°, respectively. The two joint sets both have undulating and nearly smooth surfaces, with little soil packing. Joint set 1 extends near 60 m, with fissure width of 0–3 cm; joint set 2 extends about 3–10 m, with fissure width of 0–3 cm. The stratification planes are closed. The bedding planes can be seen as joint set 3 (JS3).

Due to excavation, the rocks move slowly. During construction stage of the plants, a tension crack developed along the strike of joint sets 2, with width of 20 cm. A small-scale fast failure took place southeast of the slope. The instable block is about 10 m wide and 23 m high; the visible sliding plane length along sliding direction is more than 20 m. The failure consequently destroyed part of the new plants. By measurement for the landslide body, connecting the topographic contour map of the slope before

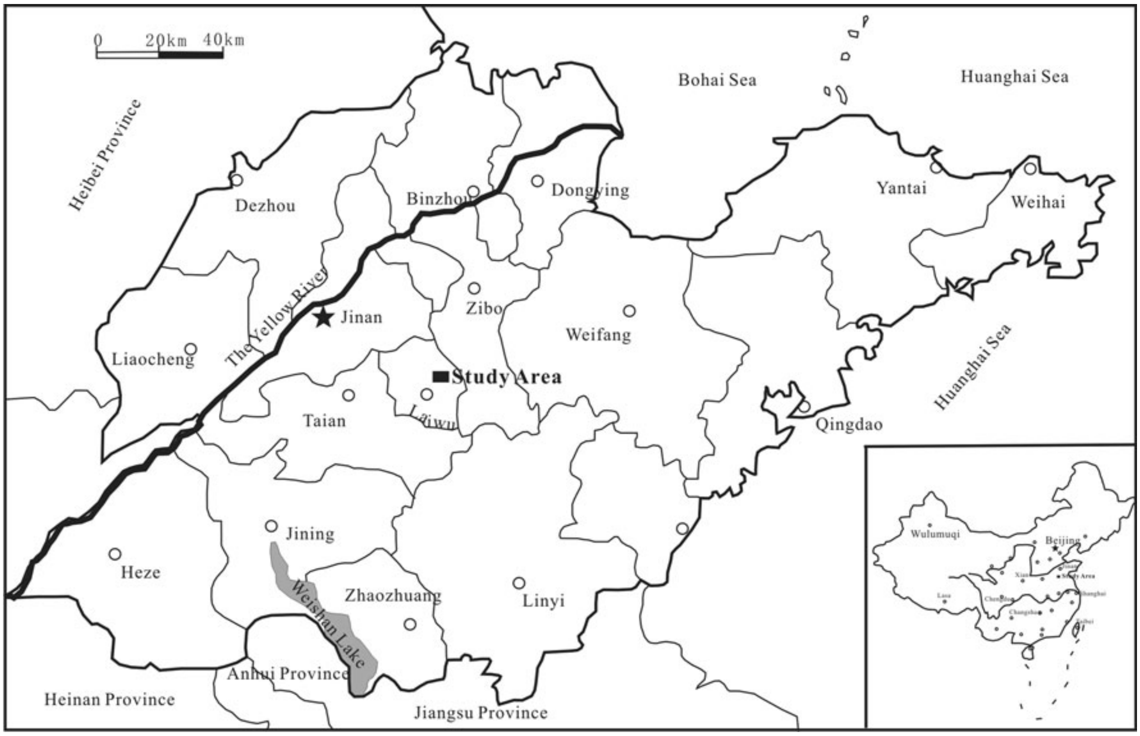

Fig. 1 Location of the landslide

failure, the section crossing the failed rock masses (Section I–I indicated in Fig. 2b) could be precisely plotted. The site investigation reveals that the sliding plane is through a relatively weak intercalated layer (Fig. 2b, c), in which the main component is clay. The weak layer gets distributed along the bedding plane in the limestone. As a result of the failure, the tension crack develops a series of little cracks along joint sets 2 (Fig. 4).

No groundwater seepage was detected through the exposed rock; therefore, it can be assumed that failure occurred at zero cleft water pressure. Furthermore, the seismogram did not indicate any activity in the vicinity of the site during slope failure. The failure may be therefore assumed to be the result of instability under static load due to gravity, which developed along the bedding plane of the clay-filled in the limestone, and has nothing to do with the groundwater and seismic activity.

In summary, the slope face dip is 70°–80° (Figs. 3, 4), with dipping direction of 30°–45°. The sliding plane is near the bedding stiff intercalated clay layer in the limestone and may be affected by the other joint set. The attitude of the clay is consistent with the limestone, white to gray, with thickness ranging between 0.1 and 0.3 m, in which the main mineral is montmorillonite, containing some calcium, with the unit weight, $\gamma_d = 19.2$ kN/m^3 (laboratory determined). The natural water content was 8–12 %, with the liquid limit (LL) 75–84 %, plastic limit (PL) 27–32 %. The permeability of the clay is poor.

It is obvious that this slope failure is along the existing geological defects/discontinuities. It can be seen from Fig. 3, JS3 strikes nearly parallel to the slope face. The dip of JS3 is smaller than the dip of the slope face and very close to the friction angle, which is 30° empirically. The tension cracks, which extend along the joint sets 2 and become the side boundary, separate the rock block from the rock mass. Additionally, the JS1 and JS2, which provide negligible resistance to failure, provide release surfaces for failure. Therefore, the above-mentioned failure of the slope was planar type. It is obvious that the failure must be along JS3.

Methods and results

Back analysis of the failed slope

The limit equilibrium methods (LEM), which are routinely adopted methods for stability calculation, are undertaken to provide a factor of safety based on a comparison of resisting forces of moments to disturbing forces or moments. In the limit equilibrium back analysis procedure, the factor of safety is equal to 1, which introduced the threshold of rupture. From the space geometry features of the exposed rock mass, the instable block includes intensely to moderately weathered limestone (the intensely weathered, $\gamma_d = 24.3$ kN/m^3; the moderately weathered,

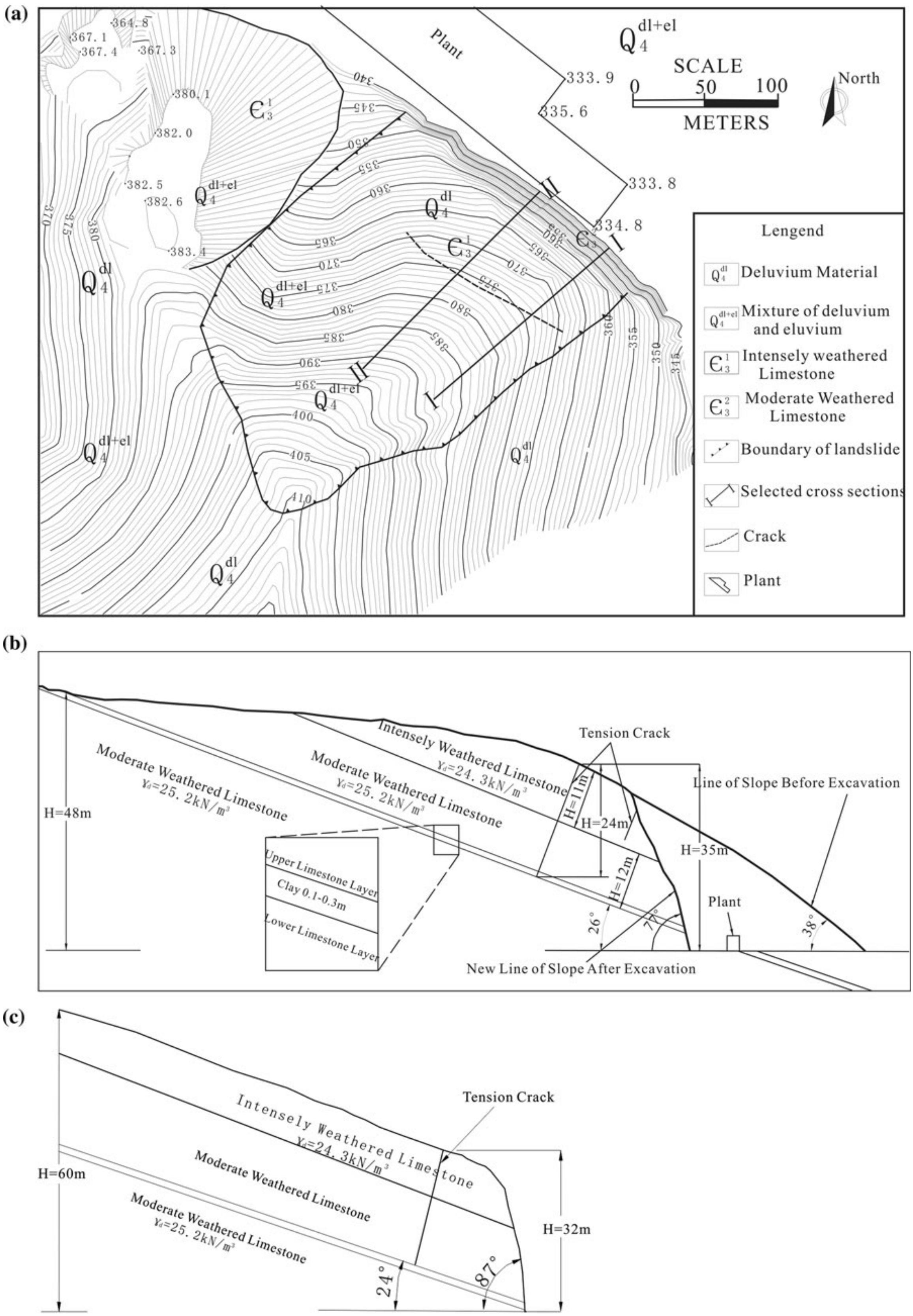

Fig. 2 **a** Engineering geological map of the failed slope. **b** Cross section I–I. **c** Selected cross section II–II

Fig. 3 Lower hemisphere equal angle stereo projection of discontinuities

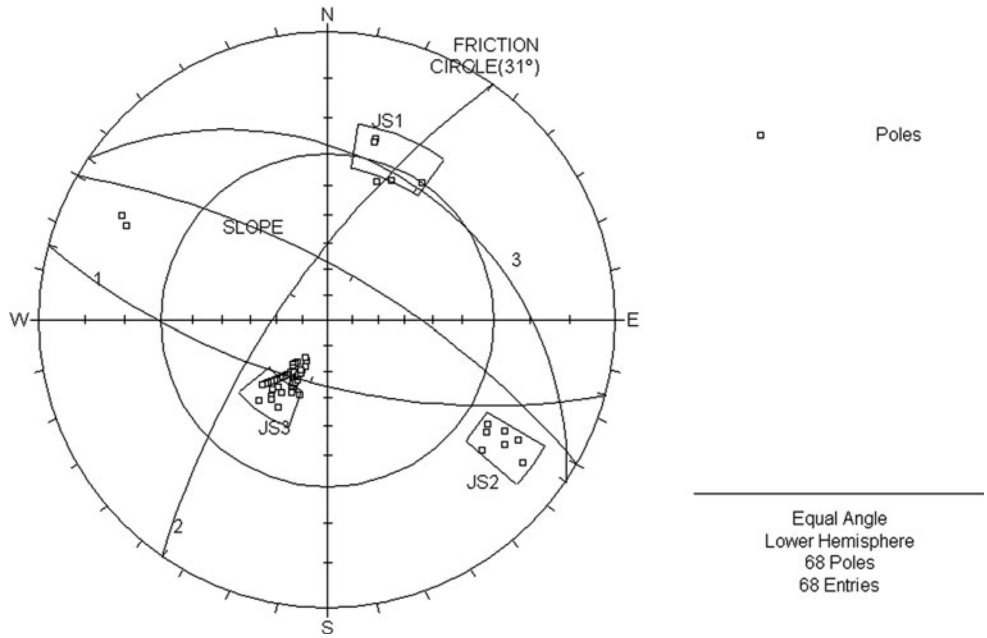

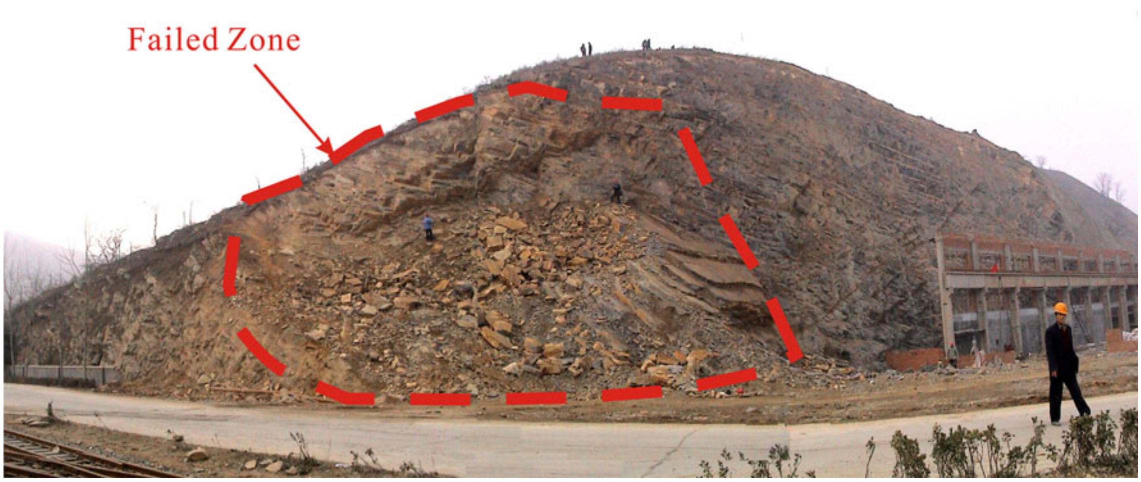

Fig. 4 The failed slope showing tension crack at the head and sliding plane

$\gamma_d = 24.3$ kN/m^3); the vertical depth of the tension crack behind the block is 24 m; it is assumed that there is no force acted on the rock block along the crack (the tension strength of the crack is 0). The sliding plane length is 31 m along bedding weak layer plane, dipping 26° into the excavation space; the sliding bed is the moderately weathered limestone.

It is obvious that the failure can be determined as planar type.

The factor of safety against single plane sliding in the general case of a saturated slope is given by (e.g., Hoek and Bray 1981):

$$F = \frac{cl + (W\ \cos\beta - U - V\ \sin\beta)\tan\varphi}{W\ \sin\beta + V\ \cos\beta} \quad (1)$$

where c is cohesion across the sliding plane (kPa); l the length of the sliding plane (m); W the overall weight of the sliding block (kN); U the resultant water force acting on the sliding plane (kN); V the resultant water force acting on the tension crack (kN); β the dip angle of the sliding plane (°); and ϕ is the friction angle of the sliding plane (°).

In this case, sliding is assumed to have taken place under dry conditions and, therefore, U and V are both zero; the calculated weight of the sliding block (W) is 14,250 kN by the careful maps; and the average dip of the sliding plane is 26°; l is 31 m. Under the state of limit equilibrium, the factor of stability is 1.0, the strength parameters (c and ϕ) of the sliding plane depend on each other, and can be described as:

$$c = \frac{W \sin\beta - W \cos\beta \tan\varphi}{l} \quad (2)$$

To back analysis the landslide, it is assumed that the ϕ of the sliding plane varies between 10° and 26°, the graphical solution for this relationship is shown in Fig. 5.

From cross section II–II plotted by site measure and geological map, the length of the sliding plane is 23.6 m, the height of the instable block is 32 m, the weight of the block is 10,133 kN. The graphical solution for c and ϕ relationship is shown in Fig. 5. Because the sizes and shapes of the sliding blocks in the two cross sections are approximative, the continuous curves is very close, though they have a intersection point, the deviation of the values from the point is easily affected by the measure and plot. For this problem, to obtain the parameters of the sliding plane, the necessary tests should be carried out.

It is shown that the maximum value of back calculated cohesion is not greater than 132 kPa. According to the site investigation, the clay is stiff; from Fig. 5, if $\phi = 10°$ (relatively low value), c must be 132 kPa, which indicates that sliding plane is in the clay. However, if $\phi = 26°$, c must be 0. For the clay, the latter of the above solution is not in reality, which means the sliding is not in the clay but in the contact between the stiff clay and the overlying or underlying limestone.

Direct shear tests on the clay

To reduce the disturbance to the samples, the samples of laboratory direct shear tests were retrieved in the field. The samples are divided into six groups, each group includes four samples. The field values of normal and shear stresses acted on the clay are calculated to be $\sigma_n = 510$ kPa, $\tau = 243$ kPa. Considering the natural stress field, four cylindrical specimens, with height of 2 cm, cross-sectional area of 30 cm^2 were saturated. After saturation, the samples were consolidated under normal stresses of 100, 200, 400, and 600 kPa. Following consolidation, the samples were sheared under drained condition, and at the horizontal displacement rate of 0.014 mm/min. The above mentioned laboratory tests for the clay are repeated six times.

The typical stress–strain curves are shown in Fig. 6. It is assumed the clay is a Mohr–Coulomb material. When the four tests yield, the normal and shear stress on the shear plane is as plotted in Fig. 7. From the resulting best linear fit, the effective cohesion and friction angle are 207.6 kPa and 17°, respectively ($R^2 = 0.993$). It is assumed that the sliding plane is in the clay; the factor of stability calculated by formula (1) is 1.66 according to the above strength parameters, whose result means the slope must be stable. Considering under high normal stress, such as 400–600 kPa, which is near the natural normal stress, $c = 230$ kPa (Fig. 7), which is close to the natural shear stress on the shear plane, $\phi = 15.4°$; the factor of stability against the sliding is 1.70, the slope must be stable too. The test results from the six groups indicate the values of c are between 192 and 246 kPa, and the values of ϕ are between 12° and 17°. The calculated values of F should be between 1.50 and 2.20.

The calculated results indicate that sliding of the failure cannot shear through the clay, which may be on the contacts between the clay and the limestone.

In situ direct shear tests on the clay–limestone contact

For the rock, it is difficult to retrieve the undisturbed samples in the field. Even if the samples can be retrieved in the field, the samples would be disturbed inevitably, the accuracy of the test results will reduce, without any doubt. To reduce the disturbance to the rock mass, the samples were artificially produced in situ, and the samples are square with the shear area of 50 cm × 50 cm (Hudson 1974–2006), the height above the

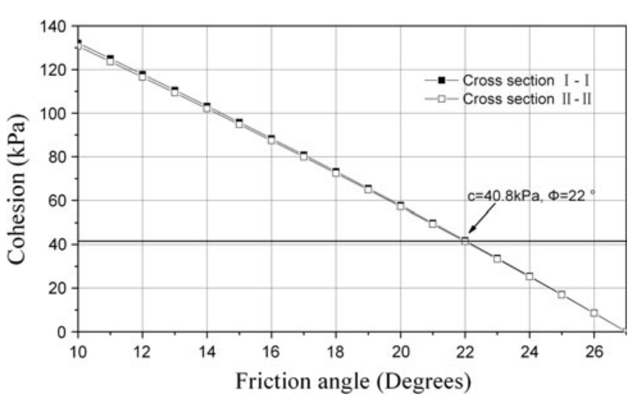

Fig. 5 Back analysis results of strength parameters of the sliding plane

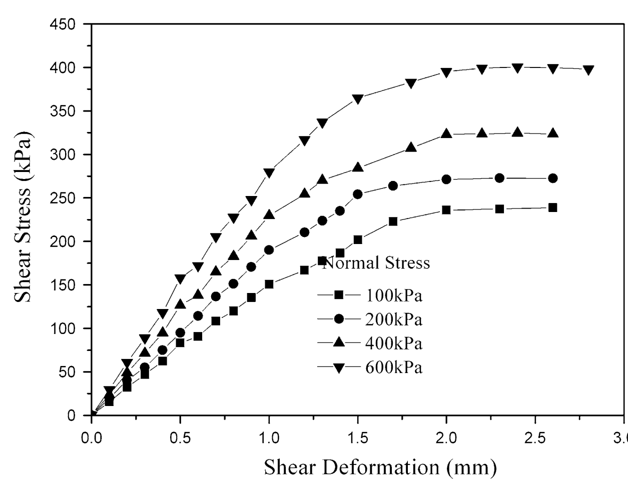

Fig. 6 Stress–strain curves for direct shear tests of the interbedded clay

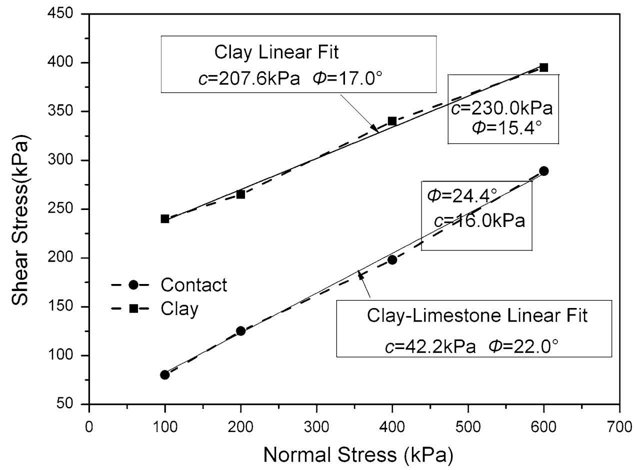

Fig. 7 Mohr–Coulomb failure envelopes for direct shear tests

Fig. 8 Equipment of shear test of clay–limestone contact

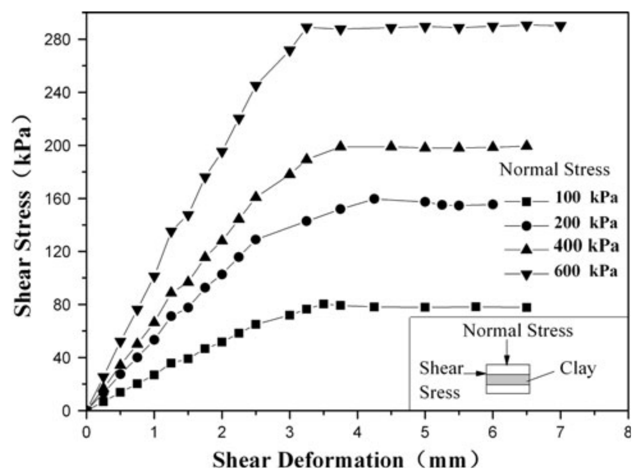

Fig. 9 Stress–strain curves for direct shear tests of the clay–limestone contact

shear plane is 40 cm, and the shear planes are set in the weak intercalated layer. To prevent the rock above the contact from being damaged or great deformation, the upper rock was packed with cement mortar, thus, being made into a regular shape (Fig. 8). The top surfaces of the sample are all flat, and paralleling with the intercalated layer. The four sides are flat and vertical to preset shear surfaces. In test processes, the shear stresses and normal stresses acted on the shear surfaces are loaded by hydraulic jacks. At the four corners, the 6 m long resin anchors were preset before tests as the anti-power of normal loading. The four dial gauge are preset (two for monitoring the vertical displacements, the other two for monitoring shear displacements), the arithmetic mean values are calculated by the monitored results of both groups. The steel boards were laid between the samples and the jacks, which can guarantee that the stress on the contact is uniform. There are two steel boards under the normal jack; the rollers were laid between the two boards for adapting to the shear deformation.

Before starting normal loading, the steel board, rollers, the other steel board, hydraulic jack, columns for transferring load and the anti-power equipments were laid in turn. As well as the shear loading, the similar components were laid in turn. After installation, the jacks were initiated to load a small amount and make the system combine closely.

There were four samples for the shear tests on the clay–limestone contact. One day before the tests, the clay was saturated; in test processes, the normal loading was divided into four grades, the next load was loaded after the previous load reached stable state. The different normal stresses acted on four samples were the same as the laboratory clay test. After the last loading, the shear stresses were loaded slowly; in shear processes, the shear stresses and shear displacements were recorded.

The stress–strain curves are shown in Fig. 9. At the same time, it is assumed the shear surfaces are Mohr–Coulomb material, when the samples yield, the relationship of the normal and shear stresses is shown in Fig. 7. The best linear fit results indicate that strength parameters are $c = 42.2$ kPa, $\phi = 22°$ ($R^2 = 0.997$), thus the factor of stability of cross section I–I calculated by formula (1) is 1.03. Considering under high normal stress, such as 400–600 kPa, $c = 16.0$ kPa, $\phi = 24.4°$ (Fig. 7), thus the factor of stability is 1.01; the two calculated results are very close to the limit equilibrium state. According to the back analysis results (Fig. 5), when the block is in limit equilibrium state, $\phi = 22°$, $c = 40.8$ kPa. The test results on the contact are consistent with the back analysis results. It can be sure that the instable block slides along the contact of clay–limestone, and the tested strength parameters ($c = 42.2$ kPa, $\phi = 22°$) of the sliding plane are reasonable.

Discussion

From the discussed results, the strength parameters of the weak intercalated layer can be decided from Table 1.

Table 1 Strength parameters of the weak intercalated layer

Parameters	Clay	Contact
c/kPa	207.6	42.2
ϕ/°	17	22

The laboratory direct shear tests indicate that the cohesion and friction angle of the filling clay are $c = 207.6$ kPa, $\phi = 17.0°$. The factor of stability of the failure is 1.66, assuming that the failure sliding through the clay, which means that the slope must be stable. For similar landslide, which sliding plane is near the relative weak layers, conventional or intuitive laboratory test methods pay more attention to the mechanics characteristics of the filling clay; this case indicates that the ideas and study methods are unconservative and misleading, because they ignore the contact of the clay–stone.

The in situ direct shear tests indicate the cohesion and friction angle of the weak intercalated layer are $c = 42.2$ kPa, $\phi = 22.0°$, which implies that the calculated factor of stability is very close to the limit equilibrium state. The test results are consistent with the back-analyzed results. Therefore, it can be sure that the shear of instable block commences along the clay-stone contact, but not through the clay.

Earlier workers (Goodman 1976; Ladanyi and Archambault 1970) found that when the infilling thickness is greater than the roughness amplitude, the shear strength of the discontinuity is controlled by the strength of the infilling. The results of this paper indicate that shear landslide may be along the contact of the clay–limestone, although the thickness of the infilling was much greater than the roughness amplitude of discontinuity. The discrepancy can be explained by the engineering properties of the stiff clay, which has high cohesion (much greater than the cohesion on contact of clay–limestone).

The shear strength of the weak plane by artificially saw-cut stone surface filled with remolded clay was tested by Hatzor (1997), whose test results are $c = 160$ kPa, $\phi = 18°$. Because of the disturbance to the stone and clay, Hatzor believes that the tested cohesion is negligible. In this study, the shear strength parameters of the contact are tested by the in situ direct tests; the samples were disturbed little; the tested parameters ($c = 42.2$ kPa, $\phi = 22°$) are close to the real situation, which indicate the cohesion is not '0' or ignorable.

Conclusion

In this study, a plane shear failure along a clay-filled bedding plane in limestone is back-analyzed by site measurement and careful geological mapping of the instable block's geometry. Then the laboratory and in situ direct shear tests for the clay infilling or the contact surface are undertaken, respectively. Thus, the material properties of the limit equilibrium are obtained. Some conclusions could be obtained:

1. To the bedding landslide along the weak layer, the earlier study results, such as Goodman (1976), Ladanyi and Archambault (1970, 1977), found that when filling thickness is greater than the roughness amplitude, the shear strength of the discontinuity is governed by the strength of the infilling. In this case, it is shown that the shear strength of the clay–limestone contact dictates the resistance force of the sliding plane rather than the strength of the clay. This discrepancy could be the result of the stiff clay. The conventional or intuitive assumption of shear failure through the clay may be erroneous or unconservative.
2. Hatzor (1997) considered that the cohesion on the clay-stone contact is negligible. However, in this study, the in situ direct shear test results, which are consistent with the back-analyzed results, indicate the cohesion is not negligible for the original structural surface.
3. In view of the characteristics of the landslide and its current stability state, it is recommended that monitoring should be undertaken to identify any displacement, and the retaining walls or appropriate reinforcement should be constructed at the front of the landslide to minimize the possibility of a catastrophic event.

Acknowledgments This paper is financially supported by National Basic Research Program of China (973 Program) (No. 2006CB403204). Zheng Quanming of Shandong Zhengyuan Construction Co., Ltd. provided great help in the field and assisted with sample preparation and direct shear testing, his careful work is acknowledged. Laiwu Iron & Steel Co., Ltd. provided free access to digitized mapping data and borehole data.

References

Alhomoud AS, Tubeileh TK (1998) Analysis and remedies of landslides of cut slopes due to the presence of weak cohesive layers within stronger formations. Environ Geol 33(4):299–311

Barton NR (1971) Estimation of in situ shear strength from back analysis of failed rock slopes. In: Proceedings of international symposium on rock mechanics, vol 1.a. Nancy, France, pp 2–27

Barton N (1973) Review of a new shear strength criterion for rock joints. Eng Geol 7:287–332

Barton NR, Bandis S (1982) Effects of block size on the shear behavior of jointed rock. In: Proceedings of the 23rd US symposium on rock mechanics, Berkeley, California, USA

Fookes P, Reeves B, Dearman W (1977) The design and construction of a rock slope in weathered slate at Fowey, South-West England. Geotechnique 27(2):533–556

Ghazvinian AH, Taghichian A (2010) The shear behavior of bedding planes of weakness between two different rock types with high strength difference. Rock Mech Rock Eng 43:69–87

Gioda G, Locatelli L (1999) Back analysis of the measurements performed during the excavation of a shallow tunnel in sand. Numer Anal Methods Geomech 23:1407–1425

Goodman RE (1976) Methods of geological engineering in discontinuous rocks. West Publishing Company, St. Paul

Goodman RE, Gen HS (1985) Block theory and its application to rock engineering. Prentice-Hall, Englewood Cliffs

Grasselli G, Egger P (2003) Constitutive law for the shear strength of rock joints based on three-dimensional surface parameters. Int J Rock Mech Min Sci 40:25–40

Haberfield CM, Johnston IW (1994) A mechanistically-based model for rough rock joint. Int J Rock Mech Min Sci Geomech Abstr 31:279–292

Hatzor ML (1997) The shear strength of clay-filled bedding planes in limestones—backanalysis of a slope failure in a phosphate mine, Israel. Geotech Geol Eng 15:263–282

Hoek E, Bray JW (1981) Rock slope engineering, 3rd edn. Institution of Mining and Metallurgy, London

Hudson JA (1974–2006) The complete ISRM suggested methods for rock characterization, testing and monitoring

Indraratna B, Haque A (2000) Shear behaviour of rock joints. Balkema, Rotterdam

Jaeger JC (1971) Friction of rocks and stability of rock slopes. Geotechnique 21:97–134

Kaiser P, Zou D, Lang P (1990) Stress determination by back analysis of excavation-induced stress changes-a case study. Rock Mech Rock Eng 23(3):185–200

Kodikara JK, Johnston IW (1994) Shear behaviour of irregular triangular rock–concrete joints. Int J Rock Mech Min Sci Geomech Abstr 31(4):313–322

Ladanyi B, Archambault G (1970) Simulation of shear behaviour of a jointed rock mass. In: Proceedings of the 11th symposium on rock mechanics. AIME, New York, pp 105–125

Ladanyi B, Archambault G (1977) Shear strength and deformability of filled indented joints. In: International symposium on the geotechnics of structurally complex formations, vol 2. AGI, Capri, pp 317–326

Maksimovic M (1996) The shear strength components of a rough rock joint. Int J Rock Mech Min Sci Geomech Abstr 33:185–200

Mostafa S, Mohsen S, Mohammad D (2010) Back analysis of an excavated slope failure in highly fractured rock mass: the case study of Kargar slope failure (Iran). Environ Earth Sci 60: 183–192

Okubo S, Nishiatsu Y (1993) Control performance of servo-controlled testing mechanics in compression and creep tests. Int J Rock Mech Min Sci Geomech Abstr 30(3):247–255

Patton FD (1966) Multiple modes of shear failure in rock. In: Proceedings of the 1st congress of ISRM, vol 1. Laboratorio rionacional de engenharia civil, Lisboa, pp 509–513

Saeb S, Amadei B (1992) Modelling rock joints under shear and normal loading. Int J Rock Mech Min Sci Geomech Abstr 29(3):267–278

Sakurai S, Takeuchi K (1983) Back analysis of measured displacements of tunnels. Rock Mech Rock Eng 16(3):173–180

Terzaghi K (1962) Stability of steep slopes on hard unweathered rock. Geotechnique 12:251–270

Zhang LQ, Yue ZQ, Yang ZF, Qi JX, Liu FC (2006) A displacement-based backanalysis method for rock mass modulus and horizontal in situ stress in tunneling—illustrated with a case study. Tunn Undergr Space Technol 21(6):639–649